Desalination and Water Treatment
www.deswater.com
doi: 10.1080/19443994.2015.1135826

57 (2016) 23473–23488
October

Taylor & Francis
Taylor & Francis Group

Preparation of an asymmetric microporous carbon membrane for ultrafiltration separation: application to the treatment of industrial dyeing effluent

Nouha Tahri[a,*], Ilyes Jedidi[a], Salwa Ayadi[a], Sophie Cerneaux[b], Marc Cretin[b], Raja Ben Amar[a]

[a]*Laboratoire Sciences des Matériaux et Environnement, Faculté des Sciences de Sfax, Route de Soukra Km 4, Sfax 3000, Tunisie, Tel. +216 21 064 024; email: tahri.nouha@yahoo.fr (N. Tahri), Tel. +216 21 449 989; email: ilyesjedidi@yahoo.com (I. Jedidi), Tel. +216 22 300 680; email: a.salwa@voila.fr (S. Ayadi), Tel. +216 21 603 013; email: raja.rekik@fss.rnu.tn (R. Ben Amar)*
[b]*Institut Européen des Membranes, UMR 5635 (CNRS-ENSCM-UM), Université de Montpellier, place Eugène Bataillon, 34095, Montpellier cedex 5, France, Tel. +33 04 67 14 91 56; email: sophie.cerneaux@umontpellier.fr (S. Cerneaux), Tel. +33 04 67 14 91 94; email: marc.cretin@umontpellier.fr (M. Cretin)*

Received 8 September 2015; Accepted 15 December 2015

ABSTRACT

An asymmetric tubular carbon membrane with an ultrafiltration microporous top layer has been prepared using thermosetting phenolic resin and carbon black (CB) as carbon precursors. The membrane was composed of a mesoporous interlayer with an average pore size of 0.6 μm deposited by slip casting process on the inner face of a macroporous support. The microporous top layer was deposited by the same process using suspensions of commercial CB powder (44 nm average pores size). An initial ultrafiltration membrane with an average pore size of 7.9 nm and a thickness of 8.34 μm was formed requiring 10 min casting time and a curing–carbonization cycle at 700˚C under nitrogen atmosphere. An approach consisting of repeating casting–carbonization cycle was adopted to correct the defects that appeared at the surface. Results showed that an UF-corrected membrane denominated UF-C_4 was successfully prepared by adding only one layer after its composition and conditions of deposition were determined. A crack-free UF membrane with a thickness layer of 12.6 μm, a mean pores size of 5.3 nm, and a molecular weight cut-off of 90 kDa was then obtained using only 6 min casting time. It was found that this membrane could be applied efficiently to the treatment of industrial dyeing effluent.

Keywords: Ultrafiltration membrane; Casting–carbonization cycle; Corrected membrane; Crack-free layer; Dyeing effluent

1. Introduction

Membrane separation is considered to be a suitable technology for the separation of various mixtures within the textile, chemical, food, and pharmaceutical industries due to advantages offered by their relatively high stability, efficiency, low energy requirement, and ease of operation [1–3]. Membranes with good thermal and mechanical stability combined with good solvent resistance are important for industrial

*Corresponding author.

processes. The growing interest in this area led to the development of inorganic and polymeric membranes.

Inorganic membranes including zeolite, silica, alumina, zirconia, and carbon membranes have emerged as promising materials to conquer the challenges and competition in current membrane-based separation technologies with excellent separation capability (through molecular sieving) for a broad range of applications [3–7]. Generally, besides having superior thermal stability and chemical resistance, inorganic membranes possess a unique feature of anti-swelling at elevated temperatures and longtime [8–11].

Carbon membranes have attracted much attention as an alternative for polymeric membranes with all the advantages of inorganic materials in addition to being chemically inert, and they tend to be much less brittle than most ceramics. Carbon membranes have also the potential to be more cost-effective for large-scale manufacturing due to the very low cost of the carbon precursors [1,12].

In recent years, microporous membrane technology has received great attention as a practical process for concentration and purification of macromolecular species in aqueous solutions [13–20]. Referring to literature, studies involving the preparation of carbon membrane for UF application are scarce and there are almost no previous works treating the elaboration of microporous carbon membrane totally on carbon (membrane support and active layer).

Microporous carbon membranes are generally produced by carbonization of various polymeric precursors [2,5,19–21]. It was found by many researchers that the phenolic resin was the excellent carbonaceous material due to its considerable fixed-carbon yield, high inherent purity and low cost.

Numerous studies were focused onto the preparation of microporous carbon membrane for gas separation by carbonizing of a phenolic resin film deposited by slip casting process on non-carbon supported membrane. One of the most important problems to be solved in preparing these membranes is related to their reproducible separation properties. Several researchers have reported that carbon membranes prepared under similar pyrolysis conditions could not exhibit the similar separation performances, especially in term of selectivity [22]. Therefore, many researchers focused their attention on the preparation of high-performance ceramic membranes using asymmetric multilayer configuration. The development of such structure includes shaping an appropriate support material, preparation of microfiltration interlayer, and then an ultrafiltration top layer [7,23–29]. Shiflett et al. [30] attempted to prepare defect-free carbon layers over porous stainless steel by repeating for four times the coating–carbonization steps of polyfurfuryl alcohol. Kita et al. [31] coated the external surface of porous alumina tubes with 40 wt.% phenolic resin solution via dip-coating method. They repeated the coating–carbonizing operations for three to four times in order to form a defect-free carbon layer. Rao and Sircar [32] coated a porous graphite with latex polyvinylidene chloride. They also repeated coating–carbonizing operations for five times.

Nevertheless, few researchers have reported that only one-time coating could be successful in the formation of defect-free carbon layer over the surface of support [33,34]. Centeno et al. [20] prepared carbon membranes via the coating of thin layers of phenolic resin over the internal surface of porous alumina tubes. Wei et al. [34] also used a tubular support made of novolac® resin particles and coated by a 60 wt.% resin solution in alcohol. They showed that only one-time coating–carbonizing operation was enough for the formation of a defect-free carbon layer.

The purpose of this paper is to demonstrate that it is possible to prepare a crack-free tubular membrane totally made from carbon material with a microporous top layer for ultrafiltration separation. The slip-casting process was adopted for the deposition of the intermediate and the top layer using a phenolic resin as carbon precursor. Casting–carbonization cycle was repeated in order to create a uniform UF layer over the entire surface and thus covers any defects in carbon layer that would seriously decrease the performances of the membrane. The application of the obtained UF membrane for the treatment of industrial dyeing effluent was performed and the result was then discussed.

2. Experimental

2.1. Materials

Mineral coal was used as the main carbon material source for preparing carbon membrane. This powder presents high carbon content, low ash content, and moderated volatile components. According to previous studies [35,36], it was found that the average pore size of carbon membrane decreases with decreasing coal particles size and then average particle sizes of 100 and 1.8 μm were selected for the preparation of the support and the microfiltration (MF) layer, respectively.

For the preparation of the UF layer, commercial carbon black (CB) powder of an average particle size of 44 nm was used instead of the mineral coal. The CB was purchased from TIMCAL Group (Switzerland).

The second source of carbon used in this work was Novolac® phenolic resin (NPR) marketed by the company Irons Resins S.A, Spain (Sumitomo Bakelite co). High carbon yield and low price are the most important benefits of NPR precursors [1]. Previous studies [36,37] showed that the carbon content in the resin represents 25% of its total molecular weight (reached at 700°C under nitrogen atmosphere). Besides its role of carbon precursor, the resin also acts as binder and porosity agent [36].

2.2. Membrane preparation

The membrane preparation involved two main steps: the production of high-quality macroporous support on which active layer was deposited. To achieve this, firstly, a macroporous carbon tube (OD/ID = 10 mm/8 mm) having a pore volume of 38% and a mean pore diameter of 9 μm was prepared by extrusion–carbonization process. For this, an extruded paste was prepared from a mixture of mineral coal powder, organic additives and an alcoholic solution of NPR. The different percentages were determined in a previous work [36]. Secondly, an intermediate MF layer was then deposited by slip casting process to sustain the final layer and to avoid the infiltration of UF suspension inside the large pores of the tube. For this, a suspension made from carbon powder (1.8 μm average particles size) and an alcoholic solution of NPR (Resin/Ethanol = 15/85 wt.%) was slip-casted on the inner face of the support for 6 min at room temperature (Table 1). MF layer with an average pore diameter of 0.6 μm and a thickness of 22 μm was obtained, thanks to a curing–carbonization cycle at 700°C under a nitrogen stream of 1 mL/min (Fig. 1)

Thirdly, active UF top layer was prepared also by slip casting process using a carbon slip made of an alcoholic solution of NPR mixed with a commercial CB powder. The mixture was homogenized by ultrasonic exposure at a power of 180 W for a maximum of 5 to 10 min to avoid resin cross-linking and then slip-casted on the inner face of the MF membrane. The deposited layer was treated following the same temperature program than that used for MF membrane preparation (Fig. 2).

Table 1
Composition of MF suspension

Component	Percentage (%)
Powder carbon (1.76 μm)	20
Alcoholic solution of NPR	80

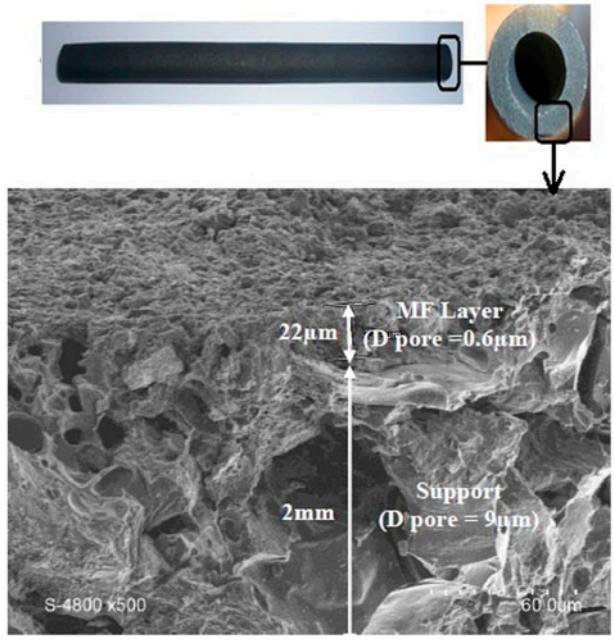

Fig. 1. Picture and SEM micrograph of the tubular carbon microfiltration membrane.

2.3. Membrane characterization

The pore volume and the average pore diameter of both support and MF intermediate layer were determined by Hg porosimetry on a Micrometrics Autopore II 9220 V3.05 apparatus.

The characteristics in terms of morphology, surface aspect, and membrane thickness were checked using scanning electron microscopy (SEM).

The hydrophobicity is one of the important properties to characterize the elaborated membranes. It can be evaluated by measuring static water contact angle. Therefore, the measurement of contact angles using ultrapure water was performed at room temperature (20°C) using an OCA 15 from Dataphysics apparatus, equipped with a CCD camera, at resolution of 752–582 square pixels, working at an acquisition rate of four images per second. The collected data were processed using OCA software. The drop image was recorded using video camera and digitalized. Each contact angle determined was the average value of 20 measurements.

2.4. Permeation properties and pores size determination

Cross-flow filtration experiments were carried out with single channel tubular membrane having an active surface area of 13.6 cm. Before each run, the membrane was conditioned in ultrapure water

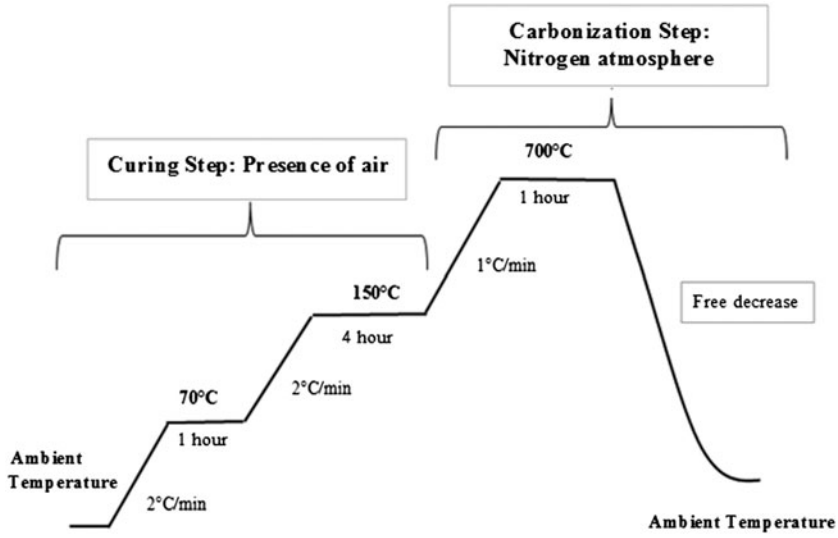

Fig. 2. Temperature–time schedule used for MF and UF membranes preparation.

(resistivity 18 M Ω cm) for 24 h to get a fast stabilization of the permeate flux. Permeability was then obtained according to the Darcy's law:

$$J_w = \mathrm{TMP}/\mu \cdot R_m \quad (1)$$

where R_m is membrane resistance, μ is water viscosity and TMP is operating transmembrane pressure (TMP).

The molecular weight cut-off (MWCO) (defined as the molecular weight of a solute retained at 90–95%) was determined for each UF membrane using 1 g/L aqueous solution of various polyethylene glycol (PEG) molecules with molecular weight ranging from 2,000 to 300 kDa. All experiments were conducted at room temperature under a TMP of 7 bar. The system was thoroughly rinsed with pure water between runs to check that membranes were not fouled during the cut-off determination.

The retention rate (R) was determined using the following classical relation:

$$R\,(\%) = 100 \times (1 - C_p/C_f)) \quad (2)$$

where C_p and C_f are the PEG solute concentrations in the permeate and in the feed solution, respectively.

Pore size distribution of the top layer was obtained from nitrogen adsorption/desorption isotherm using a Micrometrics Asap 2010. Pore diameter was estimated by BJH (Barret–Joyner–Halenda) method [38].

3. Results and discussion

3.1. Optimization of the ultrafiltration layer

Many researchers have developed technologies for the preparation of UF membranes by deposition of a microporous carbon layer on alumina supported membrane to be used in gas separation [5,17,20] or directly on a clay support to be used as nanofiltration (NF) membrane in the treatment of chromium polluted wastewater [19]. They claimed that the thickness of the top layer plays an important role in defect formation as well as in separation properties. For this, casting time and suspension's viscosity (related to the concentration of the NPR and the CB powder) are the two main parameters generally considered.

To determine the optimal viscosity of the UF suspension, different solutions have been prepared differing by the percentage of NPR and CB powder. For each composition, six casting times (from 2 to 12 min) have been tested. Samples codes were determined according to this form: UF–NPR concentration/% CB/casting time (Table 2).

Surface and cross-section morphologies of membranes achieved with different casting times were characterized by SEM. Results show that the layers formed using a casting time of 2 and 4 min led to a fine films of 0.5 to 1.1-μm thickness (result not shown). The thickness increased progressively with casting duration. When analyzing the texture of the surface, it can be concluded that the majority of samples realized with 10 min casting time showed fewer defects (cracks and pinholes) than that obtained after casting duration of 6 and 8 min.

Table 2
Different conditions tested for UF layer preparation

Concentration of NPR in alcoholic solution (wt.%)	CB powder (wt.%)	Suspension viscosity (cp)	UF membrane code
10	3	14	UF-10/3
	4	17	UF-10/4
15	3	23	UF-15/3
	4	28	UF-15/4
20	3	31	UF-20/3
	4	34	UF-20/4

Fig. 3 shows SEM micrographs of the inner surface and cross section of UF membranes prepared with 10 min casting time. It is noticed here that the SEM images are representative of the total analyzed surface by considering three samples taken from different locations on the tubular membrane.

It can be clearly observed that UF-10/3/10 and UF-10/4/10 membranes prepared from low concentration of NPR, present the highest level of defects.

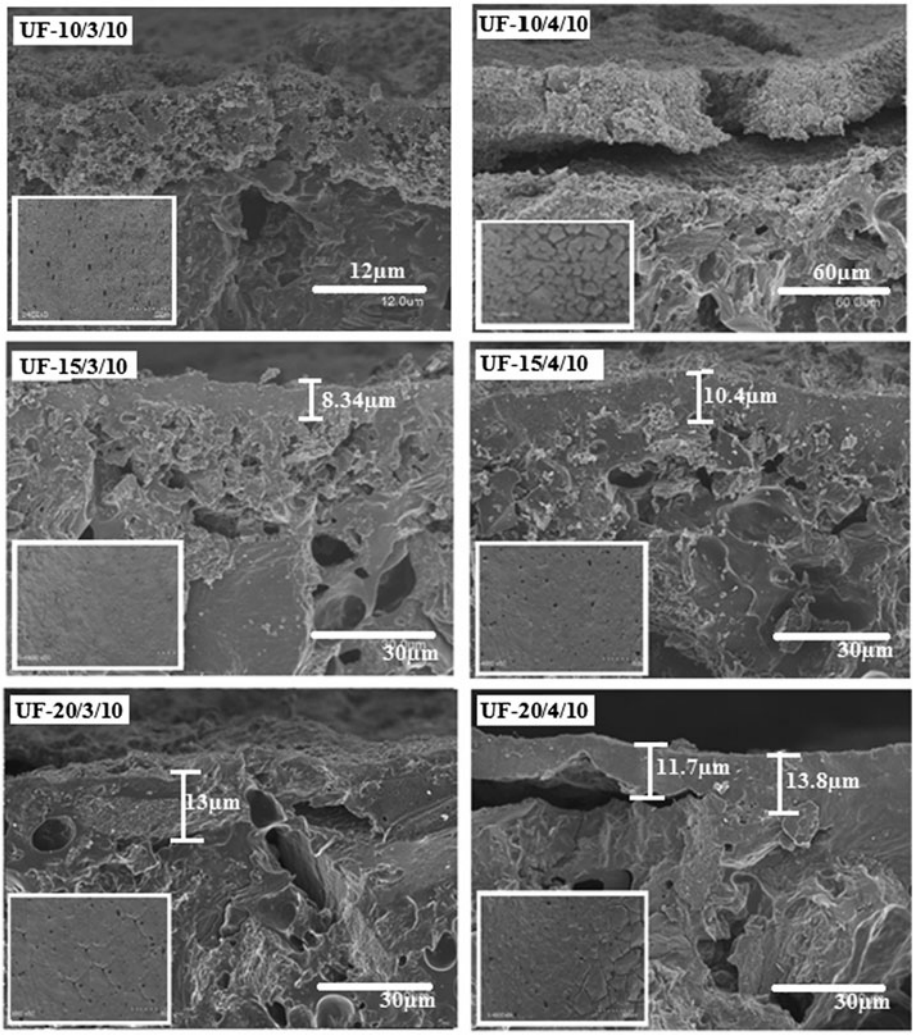

Fig. 3. SEM micrographs of UF membranes prepared at 10 min casting time for the different suspensions. Surface morphology is shown in the insert.

Therefore, the slip with low viscosity can cover easily the supported membrane and embrace all its irregularities, but it was not sufficient to maintain a homogeneous layer without defects. Thus, the composition of the suspension should be controlled to obtain the suitable layer without any defects.

When increasing the NPR concentration (membranes UF-20/3/10 and UF-20/4/10), the UF layer thickness increased and more pinholes appeared on the surface.

Therefore, it can be concluded that 15% NPR in alcoholic solution was the appropriate resin concentration for the preparation of UF layer. Considering the layer morphology in terms of thickness and surface texture, it can be seen that UF-15/3/10 membrane shows a homogenous texture with fewer defects than the membrane prepared with 4% CB.

Based on this, the best UF membrane texture was obtained for UF-15/3/10 having the following composition: 15 wt.% NPR, 3 wt.% CB powder.

When comparing the thickness and the surface morphology of membranes UF-15/3 group (having the same slip characteristics and different casting times), it is noted that the surface morphology improves with casting time until 10 min. At 12 min, the membrane presents many cracks and its thickness reached 9.3 μm, which seems to be the critical value. Indeed, Shiflett et al. [30] showed that for every combined system support/thin layer, there is a critical thickness, beyond which, cracks are formed (Fig. 4).

Therefore, it can be shown that UF-15/3 membrane made by considering 10 min as casting time, has the best structure even though a few pinholes remained. From the point of view of reproducibility at laboratory scale as well as at large scale, it will be interesting to follow a specific approach to prepare crack free membranes having similar characteristics in terms of morphology and separation performances.

3.2. Casting–carbonization cycle

From literature, it appears that the main problem, induced during the preparation of microporous carbon membrane using different carbon precursors, was the presence of cracks and pinholes that seriously decrease the performances of the membrane [22,29–32].

Different solutions have then been proposed to prevent defects formation or even to remove them whether by adjusting the synthesis technique or by choosing crack-correction methods for UF and NF membranes applied to gas or liquid separation. The main crack-correction approach used for carbon membranes was based on the repetitive casting–carbonization cycles until a correct membrane is obtained [12,39,40].

3.2.1. Determination of the correction layer number

The correction approach adopted was based on the deposition of more than one layer to correct the

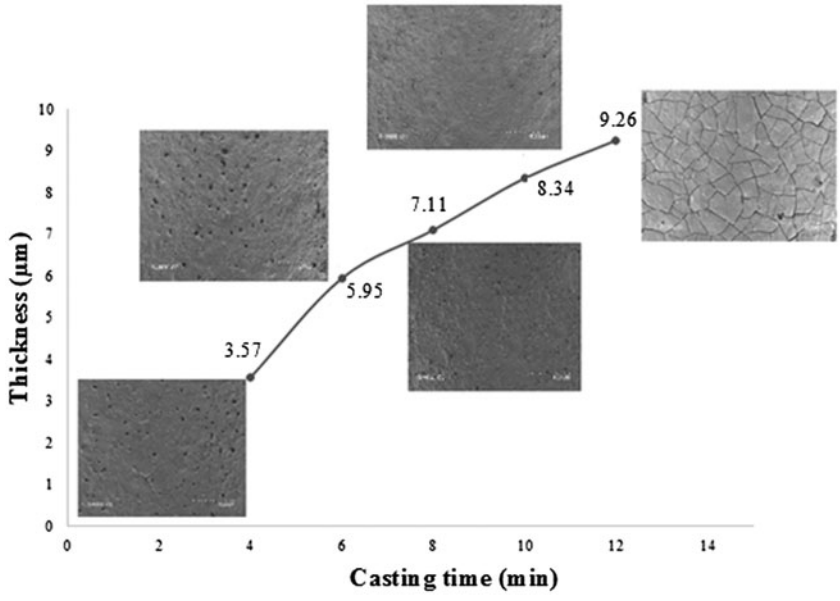

Fig. 4. Evolution of the surface morphology and the thickness of UF-15/3 with different casting times.

defects obtained with the optimized UF-15/3/10 membrane. Since the purpose of such approach is to improve the morphology of the surface and to keep the layer thickness as thin as possible, the CB powder percentage and the casting time were both reduced in each deposited layer as shown in Table 3. The following code can now be used to identify the different corrected UF membranes.

3.2.1.1. Morphology of UF layer. According to the SEM pictures from Fig. 5, it can be observed that the thickness increases with the number of layers from 8 to 26.6 μm considering, respectively, the initial optimized layer to the third corrected one. It seems also that the surface of UF-C_1 membrane (corrected with only one layer) is the most uniform and has the smoothest texture with almost no visible defects. Nevertheless, the UF-C_2 shows a multi-defects structure, which has been corrected to obtain the UF-C_3 membrane.

To optimize the number of corrected layers and to check the effectiveness of the multilayers approach used in this study, the surface and cross-section morphology data seem not sufficient. For this, multilayers UF membrane was selected based on the determination of a relationship between thickness, permeability, and average pore size.

3.2.1.2. Characterization of the multilayer UF membrane. Multilayers UF membrane was first characterized by their water permeability. A stable water flux was obtained after a few minutes of filtration and the average permeability was of 22.7, 15.25, 12, and 8.5 L/h m^2 bar^1 for UF, UF-C_1, UF-C_2, and UF-C_3, respectively. Deposition of one, two, and three correction layers over the initial UF membrane led to a decrease in the membrane permeability by 33, 47, and 62%, respectively.

There are two reasons to account for this trend: the membranes thickness and the average pores size. Indeed, the membrane thickness increases by 2, 3, and 4 times with respect to the number of layers deposition (one, two, and three layers, respectively) over the initial layer. The thicker the membrane is, the lower the permeability is (Fig. 6). Similar results were obtained by Strano et al. [39,40], when preparing nanoporous carbon membrane with pores in the UF range. They demonstrated that the low permeability was a direct result of the large thickness of the selective layer (up to 15 μm) produced by a multiple layer deposition.

The variation of the retention rates for increasing molecular weight of PEG molecules is shown in Fig. 7. All membranes displayed similar trends: the retention increases progressively with the molecular weight of PEG, then stabilized when the membrane retained 90% or more of solute. It is difficult to obtain the absolute cut-off for the membrane because it depends on the nature as well as on the conformation of the polymer used for the filtration tests [19]. The cut-off of UF, UF-C_1, UF-C_2, and UF-C_3 membranes determined from the PEG filtration are approximately 120, 79, 72, and 59 kDa, respectively. The slight variation of the MWCO from 79 to 72 kDa when one and two correction layers, respectively, were deposited can be attributed to the apparition of cracks and pinholes in the second correction layer before the addition of the third. Therefore, during filtration tests, the first correction layer is the active one. These results affect greatly the membrane permeability.

The decrease in MWCO with the number of the correction layer can be explained by the elimination of pinholes that affect the performances of the membrane as well as the decrease in the membrane pores size.

The determination of UF pores size was done using adsorption/desorption isotherm of N_2 at 77 K. Results show that all the manufactured UF membranes exhibit a type I adsorption isotherm according to IUPAC, which is associated with microporous structure. The adsorption equilibrium was established at a very low relative pressure. The slight gain in uptake at the end ($p/p_0 \sim 1$) can be attributed to the presence of mesopores or macropores (Fig. 8).

The average pore diameter as well as the different characteristics of the initial and corrected membranes are summarized in Table 4. It can be observed that the increase in the layer number from one to three led to

Table 3
Variation of CB powder percentage and casting time with the number of deposit layer

Layers	Code	Concentration of NPR in alcoholic solution (wt.%)	CB powder percentage (wt.%)	Suspension viscosity (cp)	Casting time (min)
Initial optimized layer UF-15/3/10	UF	15	3	23	10
1st corrected layer	UF-C_1	15	2.5	18	6
2nd corrected layer	UF-C_2	15	2	15.3	3
3rd corrected layer	UF-C_3	15	1.5	13.7	2

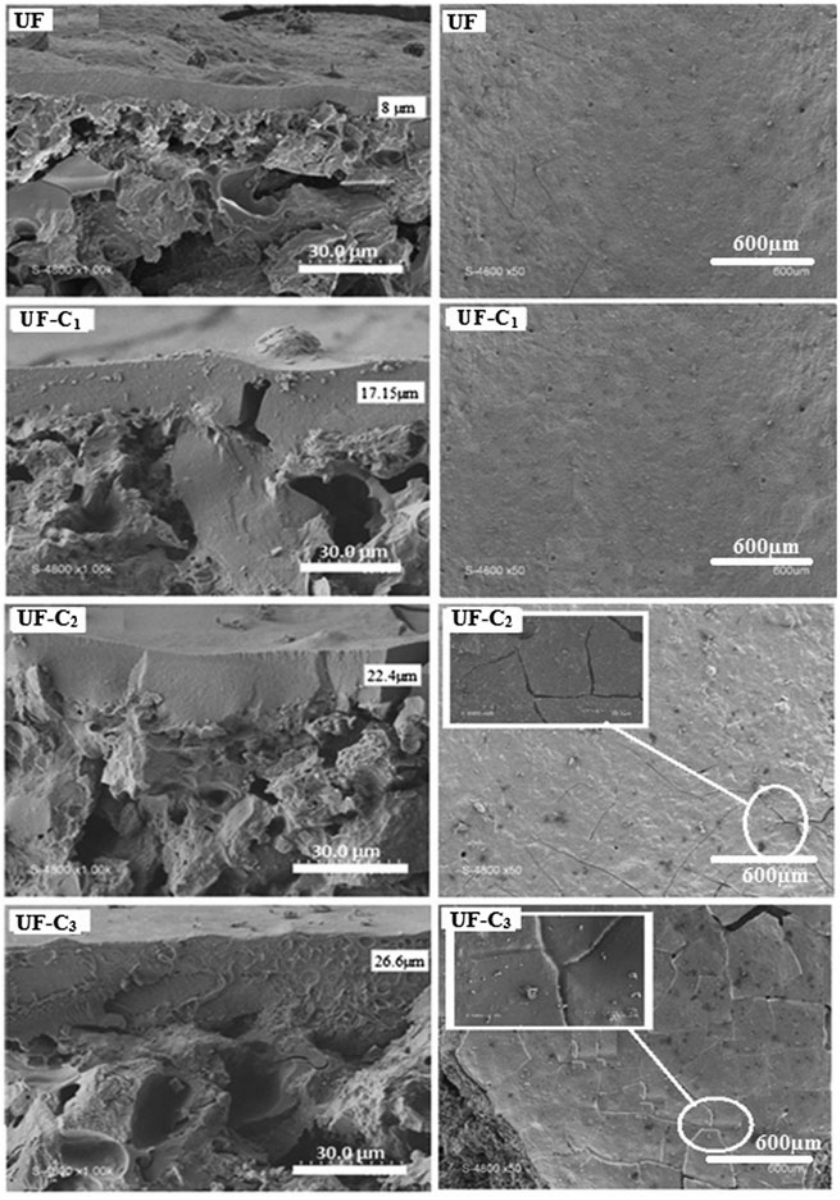

Fig. 5. Evolution of the surface morphology and the thickness of the initial and corrected UF membranes.

an increase in the membrane thickness from 17.15 to 26.6 µm as well as a decrease in the pores size from 4.8 to 3.5 nm, respectively. Consequently, the membrane permeability decreased from 15.25 to 8.5 L/h m^2 bar.

To estimate the hydrophobicity/hydrophilicity character of the different UF membranes, water contact angle was determined. This measurement can help qualitatively assessing each layer's wettability. Generally, contact angles more than 90˚ ± 2˚ indicate significant hydrophobicity, while lower contact angles, i.e. less than this value, indicate increasing hydrophilicity [41–43].

In our case, water contact angle increased slightly when corrected layers were added from 106˚ ± 2˚ for initial UF membrane to a mean value of 111˚ ± 3˚ whatever the layer number. This result confirms hydrophobic character of carbon membranes previously found [36].

3.2.1.3. Determination of the membranes resistance. Taking into account, the series resistance model (Eq. (1)), the determination of the membrane resistances (R_m) was illustrated in Fig. 9. It can be seen that R_m increased linearly with the number of the deposited

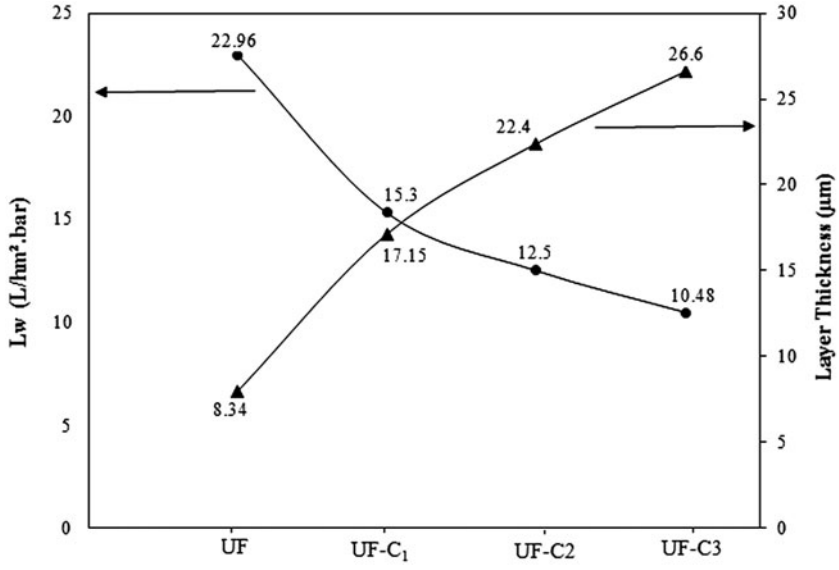

Fig. 6. Evolution of water permeability and layer thickness between the initial and the corrected UF membranes.

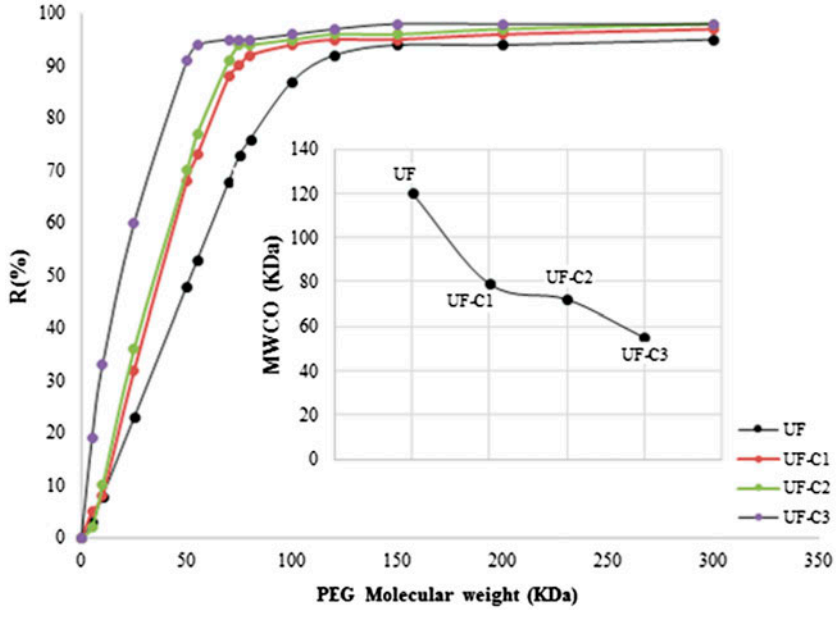

Fig. 7. Variation of the retention rate with increasing PEG molecular weight for the initial and corrected UF membranes.

layers until the third one and then increased drastically. Consequently, based on this result, a number of three layers can be acceptable to obtain a corrected UF membrane. However, from Fig. 5, membrane UF-C_2 presents cracks and pinholes. For this, the casting–carbonization cycle was repeated once and only one corrected layer was considered.

3.2.2. Determination of the deposition conditions of the corrected layer

Previous results showed that it could be possible to prepare a crack-free microporous UF carbon membrane with correction of the initial membrane by only one layer. It was found also that the composition of

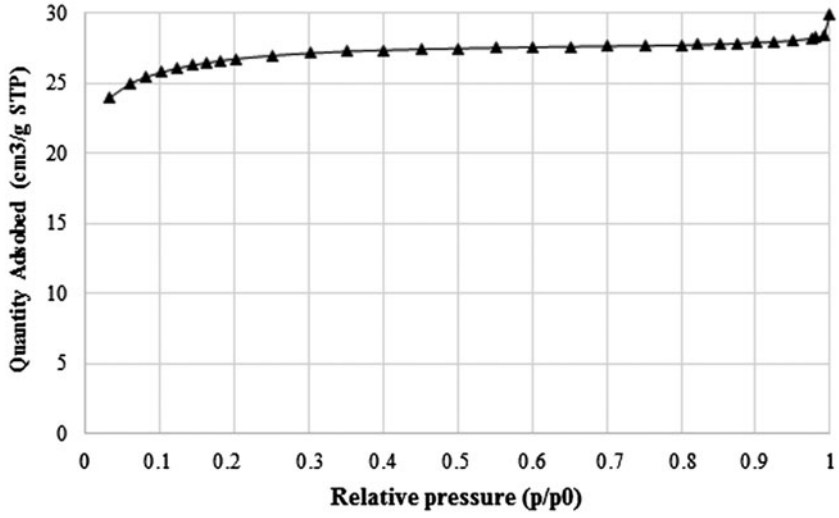

Fig. 8. Nitrogen adsorption/desorption isotherm of the UF membranes.

Table 4
Characteristics of the initial and corrected UF membranes

Membrane	Thickness (μm)	Permeability (L/h m^2 bar)	Membrane pores size (nm)	MWCO (kDa)
Initial membrane UF	8.34	22.7	7.9	120
UF-C_1	17.15	15.25	4.8	79
UF-C_2	24.4	12	4.2	72
UF-C_3	26.6	8.5	3.5	59

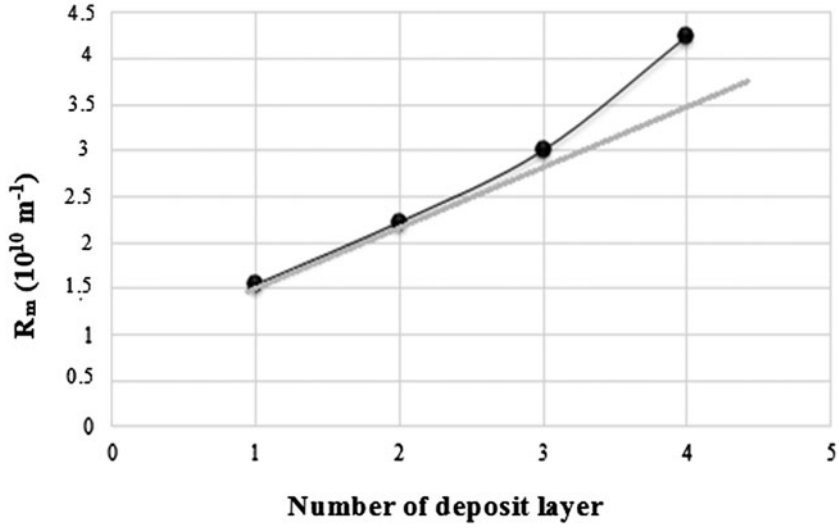

Fig. 9. Evolution of the membrane resistance with the number of deposited layers.

UF-C_1 active layer led to a good results relating to the surface morphology but led to the formation of a thick layer having a thickness of 17.15 μm. While, the composition of UF-C_3 top layer allowed the best correction by covering completely all the defects without a considerable increase in the thickness. Therefore, a new UF membrane with only one corrected layer was prepared by considering the composition of UF-C_3 top layer (15 wt.% NPR, 1.5% CB powder). For a best adhesion of the layer on the supported membrane, the suitable casting time was determined. For this, a casting time varying from 2 to 6 min was applied.

Fig. 10 represents the variation of the surface morphology of the new corrected membrane, named UF-C_4, with the different casting time.

It can be observed that the surface texture was improved by the increase in casting time and the best texture was obtained at 6 min with a thickness of 12.6 μm and an average pore size of 5.3 nm.

Considering the previous results relating to the composition of the different corrected layer, it can be concluded that when only one corrected layer was considered, UF-C_4 membrane presents better texture (homogenous, smooth, and defect-free surface) than UF-C_1 membrane. Table 5 shows the characteristics of the different UF membranes elaborated.

Taking into account, the layer thickness, it seems that the top layer of UF-C_4 membrane exhibits the good thickness value of 12.6 μm for ultrafiltration layer, compared with that of UF-C_1membrane of 17.15 μm. Referring to the literature [41–43], the best performances of UF membranes were obtained when the thickness didn't exceed 15 μm.

On the other hand, the increase in the membrane permeability from 15.25 to 18.8 L/h m^2 bar, respectively, for UF-C_1 and UF-C_4 membranes was due to the increase in the average pores size.

It can be noticed also that for UF-C_1, the higher viscosity of the suspension in comparison with that of UF-C_4, respectively, of 18 and 13.7 cp, leads to the formation of a dense and thicker layer. Therefore, the suspension having the lower viscosity allows mainly the correction of the defect previously appeared to obtain a thin and smooth layer.

Based on these results related to surface morphology, thickness, permeability, MWCO, and pores size, it can be concluded that the following composition of the casting suspension of 15 wt.% NPR and 1.5 wt.% CB powder, is suitable for the deposition of a correction layer using 6 min casting time. Thus, the definitely UF membrane (UF-C_4) has the following characteristics: average pores size: 5.3 nm, MWCO: 90 KDa, thickness: 12.6 μm

3.3. Application to the treatment of a real dyeing effluent

3.3.1. Wastewater characterization

The study was conducted with a real dyeing effluent supplied from a Tunisian textile factory. Dyeing processes generate a huge amount of wastewater because the production lines have to be washed out at each step during the dyeing cycle. The composition of the dye bath is generally very complex with solid particles, dyeing auxiliaries, hydrolyzed reactive dyes, substantial quantities of alkalis, and very high concentration of salt (Table 6). For this, preliminary treatment was carried out by gravity settling to remove the solid particle followed by normal filtering (filter paper with pore size of about 1 mm).

3.3.2. Ultrafiltration treatment

The UF-C_4 membrane has been applied to the treatment of the pretreated dyeing effluent. The filtration performances were conducted at ambient temperature and a velocity of 5.6 m/s.

The evolution of the permeate flux with time at TMP varying from 4 to 9 bar was illustrated in Fig. 11. Results show that, whatever the pressure used, the permeate flux decreased slightly with time to obtain a steady state value after 20 min of filtration. The stabi-

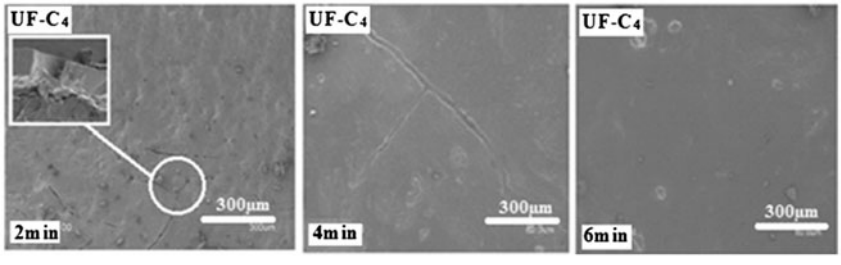

Fig. 10. Variation of the surface morphology of UF-C_4 the new corrected membrane with casting time.

Table 5
Characteristics of the different UF membranes elaborated

Membrane	Thickness (μm)	Permeability (L/h m^2 bar)	Average pores size (nm)	MWCO (kDa)
Initial UF membrane	8.34	22.7	7.9	120
UF-C_1	17.15	15.26	4.8	79
UF-C_4	12.6	18.72	5.3	90

Table 6
Principle physico-chemical characteristics of the textile wastewater

Parameters	pH	Turbidity (NTU)	Salinity (g/l)	DCO (mg/l)	Color[a]
Values	11	900	14.7	2,800	2.57

[a]Integral of the absorbance curve in the whole visible range (400–800 nm).

lized flux values increased from 7 to 16 L/h m^2 when the pressure increased from 4 to 9 bars, respectively. At 7 bars, the permeate flux was of 13.5 L/h m^2.

The permeate flux decline with time is a typical behavior of UF membrane process and can be interpreted mostly in terms of concentration polarization and fouling due to the interaction between membrane material and feed solution.

From Fig. 12, it can be observed that the retention of the different pollutants increased with pressure from 4 to 7 bar and then stabilized. From 7 to 9 bars, results showed good performances with a total retention of color and turbidity and a great retention of salinity and COD of 45 and 75%, respectively. Taking into account the COD value of 784 mg/l (corresponding to 72% of retention rate), which is below the limit value of 1,000 mg/l fixed by Tunisian legislations, the treated water can be discharged into the municipal sewerage.

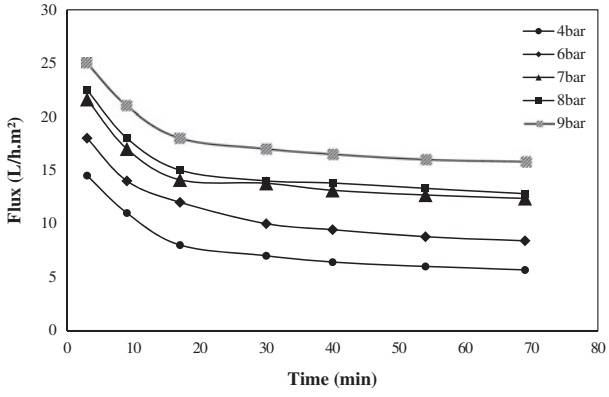

Fig. 11. Evolution of permeate flux with time at different TMP.

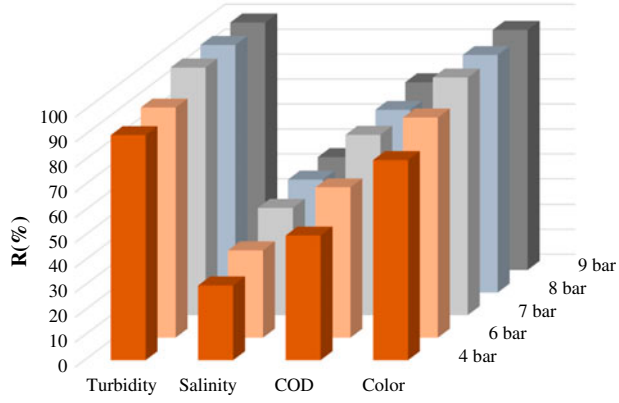

Fig. 12. Evolution of the pollutants retention at different TMP.

According to these results in terms of permeate flux and pollutants retention, a TMP of 7 bar seems suitable for this application.

3.3.3. Determination of fouling nature

Membrane fouling was caused by inorganic or organic compounds, colloids, bacteria, or suspended solids. Fouling can lower the permeate flux and might influence the retention of many compounds. It can be reversible or irreversible. Reversible fouling can be removed easily by water rinsing or changing some process parameters, while irreversible fouling is difficult to remove and might require chemical cleaning [44]. Previous works showed that reversible and irreversible fouling can contribute up to 18% and 26–46% of permeate flux reduction, respectively [45].

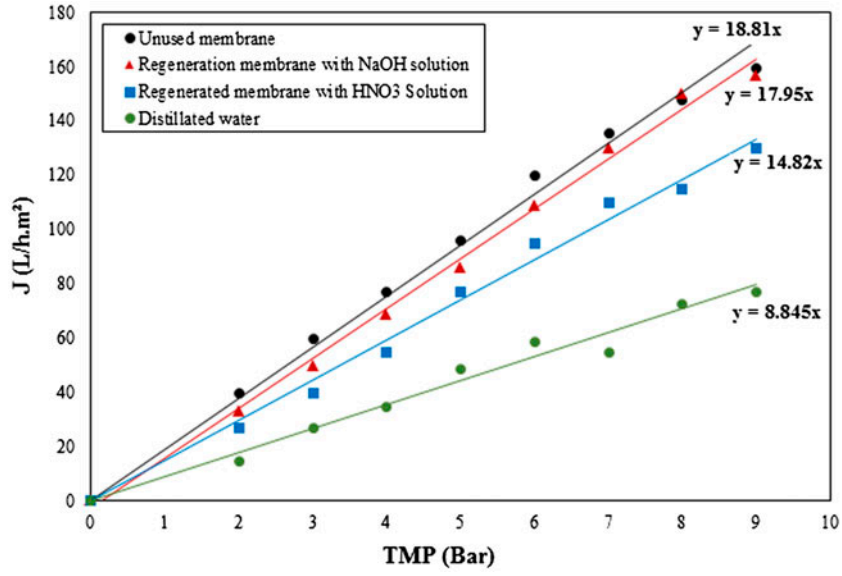

Fig. 13. Evolution of water permeate flux of unused and regenerated membranes.

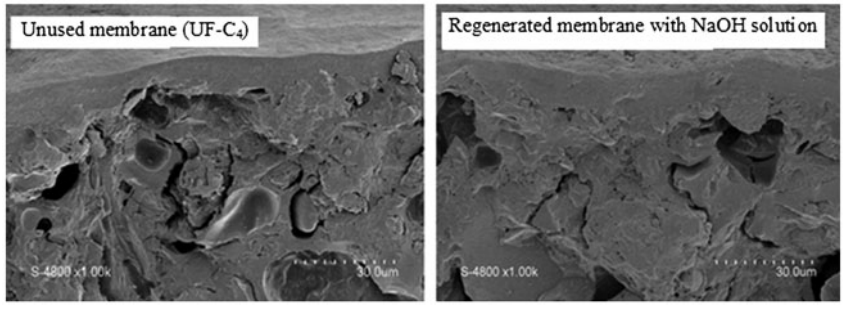

Fig. 14. SEM micrographs of unused and regenerated UF-C_4 membranes.

In order to determinate the nature of the fouling, the resistance-in-series model can be used:

$$R_T = R_m + R_{irrev} + R_{rev} \quad (3)$$

where R_T is the total filtration resistance which represents the distribution of the different partial resistances. R_m is the inherent hydraulic resistance of a clean membrane (m^{-1}), it was given by the determination of pure water permeability. R_{rev} is mainly due to the concentration polarization and deposition of retained substances on the membrane surface. It can be removed by simple water rinsing of the membrane after each filtration experiment. The R_{irrev} is the irreversible resistance resulting from the contributions of the fouling such as pore blocking and adsorption onto the membrane surface and pores, and therefore, it cannot be removed by a simple water rinsing. A specific cleaning is necessary in this case to found the initial performances of the membrane.

In our case the different resistance values are: $R_T = 1.82.10^{11}\ m^{-1}$, $R_m = 1.9.10^{10}\ m^{-1}$, $R_{irrev} = 1.12.10^{11}\ m^{-1}$, and $R_{rev} = 5.6.10^{10}\ m^{-1}$. Then, the dominant fouling mechanism can be estimated from the above results. It was found that $R_{rev} < R_{irrev}$ which indicates that the permeate flux decline is mainly due to irreversible fouling.

3.3.4. Membrane regeneration

The application of the UF membrane is limited by the inevitable phenomena of irreversible fouling which causes permeate flux decline and then represents a serious obstacle for the performances of membrane separation. The fouling phenomenon is explained in general by the hydrophilic–hydrophobic interactions between

membrane surfaces and permeate [46]. In this case, the hydrophobic membrane fouling observed during the dyeing effluent treatment is attributed to the absence of hydrogen bonding interactions at the membrane interface level. To overcome this obstacle, many efforts have been made related to membrane regeneration and results have shown that the cost of ultrafiltration is raised by cleaning process to remove fouling substances [47]. For this, a series of experiments of cleaning procedure has been carried out to regenerate the membrane using distillated water, basic solution of NaOH (pH 8.3), and acidic solution of HNO_3 (pH 3.5).

The efficiency of the membrane regeneration was determined by checking the water permeability. Fig. 13 represents the evolution of water permeate flux in presence of unused and regenerated membranes. It can be observed that water permeability of the regenerated membrane with NaOH (pH 8.3) solution was quite similar to that obtained with unused membrane (17.95 L/h m^2 bar against 18.80 L/h m^2 bar). The water permeability of the regenerated membrane with distillated water by one side and with HNO_3 solution by other side was lower than when basic solution was used (a decreased of 53 and 22% respectively were observed). In general, the chemical cleaning with basic solution serves especially to remove organic matter [48] and with acidic solution for removing mineral deposits [49]. Therefore, it seems that our membrane was more affected by organic matters that explain the efficiency of the basic solution regeneration. Fig. 14 confirms this result and shows that the same membrane texture was obtained after the membrane regeneration with NaOH solution.

4. Conclusion

New tubular asymmetric ultrafiltration membrane totally based on carbon has been prepared using NPR as carbon precursor. The carbon mesoporous interlayer and the top layer were deposited by slip casting process using suspension made from a mixture of carbon powder and an alcoholic solution of NPR followed by a curing–carbonization step.

Results show that it can be possible to prepare a crack-free microporous UF carbon membrane with correction of the initial prepared UF membrane by addition of only one layer. UF membrane denominated UF-C_4 was then prepared using a casting suspension having the following composition: 15 wt.% NPR and 1.5 wt.% CB powder. A casting time of 6 min lead to a layer thickness of 12.6 μm, which is an acceptable value for a standard UF layer (did not exceed 15 μm). The pore size and MWCO were of 5.3 nm and 90KDa, respectively.

As environmental protection becomes a global concern and with the strict Tunisian legislations and regulations that impose high limit pollution values for discharge into municipal wastewater treatment plants or into the environment, industries have to find appropriate solutions to effectively treat their effluent and eventually reuse them. This study revealed that an acceptable water quality using new prepared carbon UF membrane at affordable costs. The best performances were achieved at a TMP of 7 bar with a permeate flux of 13.5 L/h m^2. A quasi-total retention of color and turbidity was obtained while the retention of COD and salinity were of 72 and 43%, respectively. The treated wastewater can be discharged into the municipal sewerage and can be also recycled back into the process in the textile industry for washing process.

Acknowledgments

The authors are grateful for the financial support provided by the Ministry of Higher Education and Research, Tunisia. Authors would like also to thank the European Institute of Membrane, Montpellier, for providing SEM Analysis.

Nomenclature

CB	—	carbon black
C_p	—	permeate concentration
C_f	—	feed solution concentration
J_w	—	water flux
L_w	—	water permeability
MF	—	microfiltration
MWCO	—	molecular weight cut-off
NF	—	nanofiltration
NPR	—	novolac-phenolic resin
PEG	—	polyethylene glycol
R	—	retention
R_m	—	membrane resistance
R_{rev}	—	reversible resistance
R_{irrev}	—	irreversible resistance
SEM	—	scanning electron microscopy
TMP	—	transmembrane pressure
UF	—	ultrafiltration

References

[1] S.M. Saufi, A.F. Ismail, Fabrication of carbon membranes for gas separation—A review, Carbon 42 (2004) 241–259.
[2] A.F. Ismail, L.I.B. David, A review on the latest development of carbon membranes for gas separation, J. Membr. Sci. 193 (2001) 1–18.
[3] S.T. Pei, Y.L. Huey, C.O. Rui, C. Tai-Shung, Carbon molecular sieve membranes for biofuel separation, Carbon 49 (2011) 369–375.

[4] K. Li, Ceramic Membranes for Separation and Reaction, Wiley, Chichester, England; Hoboken, NJ, 2007.
[5] T.A. Centeno, A.B. Fuertes, Carbon molecular sieve membranes derived from a phenolic resin supported on porous ceramic tubes, Sep. Purif. Technol. 25 (2001) 379–384.
[6] J. Dong, Y.S. Lin, W. Liu, Multicomponent hydrogen/hydrocarbon separation by MFI-type zeolite membranes, AIChE J. 46 (2000) 1957–1966.
[7] L. Lin, S. Chengwen, J. Huawei, Q. Jieshan, W. Tonghua, Preparation and gas separation performance of supported carbon membranes with ordered mesoporous carbon interlayer, J. Membr. Sci. 450 (2014) 469–477.
[8] S.L. Wee, C.T. Tye, S. Bhatia, Membrane separation process—Pervaporation through zeolite membrane, Sep. Purif. Technol. 63 (2008) 500–516.
[9] B.H. Jeong, E.M.V. Hoek, Y.S. Yan, A. Subramani, X.F. Huang, G. Hurwitz, A.K. Ghosh, A. Jawor, Interfacial polymerization of thin film nanocomposites: A new concept for reverse osmosis membranes, J. Membr. Sci. 294 (2007) 1–7.
[10] T. Uragami, K. Okazaki, H. Matsugi, T. Miyata, Structure and permeation characteristics of an aqueous ethanol solution of organic−inorganic hybrid membranes composed of poly(vinyl alcohol) and tetraethoxysilane, Macromolecules 35 (2002) 9156.
[11] L.Y. Lu, H.L. Sun, F.B. Peng, Z.Y. Jiang, Novel graphite-filled PVA/CS hybrid membrane for pervaporation of benzene/cyclohexane mixtures, J. Membr. Sci. 281 (2006) 245.
[12] N.S. Tapan, C.F. Henry, A.L. Zydney, Development and characterization of nanoporous carbon membranes for protein ultrafiltration, J. Membr. Sci. 295 (2007) 40–49.
[13] K. Moons, B.V. Der Bruggen, Removal of micropollutants during drinking water production from surface water with nanofiltration, Desalination 199 (2006) 245–247.
[14] J.L. Acero, F.J. Benitez, F.J. Real, C. García, Removal of phenyl-urea herbicides in natural waters by UF membranes: Permeate flux, analysis of resistances and rejection coefficients, Sep. Purif. Technol. 65 (2009) 322–330.
[15] J. Fang, G. Qin, W. Wei, X. Zhao, Preparation and characterization of tubular supported ceramic microfiltration membranes from fly ash, Sep. Purif. Technol. 80 (2011) 585–591.
[16] F.K. Katsaros, T.A. Steriotis, A.K. Stubos, A. Mitropoulos, N.K. Kanellopoulos, S. Tennison, High pressure gas permeability of microporous carbon membranes, Microporous Mater. 8 (1997) 171.
[17] A.B. Fuertes, D.M. Nevskaia, T.A. Centeno, Carbon composite membranes from Matrimid® and Kapton® polyimides for gas separation, Microporous Mesoporous Mater. 33 (1999) 115–125.
[18] M.B. Shiflett, H.C. Foley, On the preparation of supported nanoporous carbon membranes, J. Membr. Sci. 179 (2000) 275–282.
[19] N. Kishore, S. Sachan, K.N. Rai, A. Kumar, Synthesis and characterization of a nanofiltration carbon membrane derived from phenol–formaldehyde resin, Carbon 41 (2003) 2961–2972.
[20] T.A. Centeno, J.L. Vilas, A.B. Fuertes, Effects of phenolic resin pyrolysis conditions on carbon membrane performance for gas separation, J. Membr. Sci. 228 (2004) 45–54.
[21] X. Zhang, H. Hu, Y. Zhu, S. Zhu, Effect of carbon molecular sieve on phenol formaldehyde novolac resin based carbon membranes, Sep. Purif. Technol. 52 (2006) 261–265.
[22] P.J. Williams, W.J. Koros, Gas separation by carbon membranes, in: N. Li, A.G. Fane, W.S. Ho, T. Matsura (Eds.), Advanced Membrane Technology and Applications, John Wiley & Sons, Inc., 2008.
[23] A. Larbot, S. Alami-Younssi, M. Persin, J. Sarrazin, L. Cot, Preparation of a γ-alumina nanofiltration membrane, J. Membr. Sci. 97 (1994) 167–173.
[24] J. Luyten, J. Cooymans, C. Smolders, S. Vercauteren, E.F. Vansant, R. Leysen, Shaping of multilayer ceramic membranes by dip coating, J. Eur. Ceram. Soc. 17 (1997) 273–279.
[25] F. Shojai, T. Mäntylä, Monoclinic zirconia microfiltration membranes: Preparation and characterization, J. Porous Mater. 8 (2001) 129.
[26] T.V. Gestel, C. Vandecasteele, A. Buekenhoudt, C. Dotremont, J. Luyten, R. Leysen, B.V. Der Bruggen, G. Maes, Alumina and titania multilayer membranes for nanofiltration: Preparation, characterization and chemical stability, J. Membr. Sci. 207 (2002) 73–89.
[27] H.J. Lee, M. Yoshimune, H. Suda, K. Haraya, Gas permeation properties of poly(2,6-dimethyl-1,4-phenylene oxide) (PPO) derived carbon membranes prepared on a tubular ceramic support, J. Membr. Sci. 279 (2006) 372–379.
[28] C.J. Anderson, S.J. Pas, G. Arora, S.E. Kentish, A.J. Hill, S.I. Sandler, G.W. Stevens, Effect of pyrolysis temperature and operating temperature on the performance of nanoporous carbon membranes, J. Membr. Sci. 322 (2008) 19–27.
[29] M. Mahdyarfar, T. Mohammadi, A. Mohajeri, Defect formation and prevention during the preparation of supported carbon membranes, New Carbon Mater. 28 (2013) 369–377.
[30] M.B. Shiflett, H.C. Foley, Reproducible production on nanoporous carbon membrane, Carbon 39 (2001) 1421–1446.
[31] H. Kita, K. Nanbu, H. Maeda, K.O. kamoto, Gas separation and pervaporation through microporous carbon membrane derived from phenolic resin, in: I. Pinnau, B.D. Freeman (Eds.), Advanced Materials for Membrane Separations, American Chemical Society, 2004.
[32] M.B. Rao, S. Sircar, Nanoporous carbon membranes for separation of gas mixtures by selective surface flow, J. Membr. Sci. 85 (1993) 253–264.
[33] X. He, M.B. Hägg, Hollow fiber carbon membranes: Investigations for CO_2 capture, J. Membr. Sci. 378 (2011) 1–9.
[34] W. Wei, S. Xia, G. Liu, X. Gu, W. Jin, N. Xu, Interfacial adhesion between polymer separation layer and ceramic support for composite membrane, AI. Chem. Eng. J. 56 (2010) 1584–1592.
[35] C. Song, T. Wang, Y. Pan, J. Qiu, Preparation of coal-based microfiltration carbon membrane and application in oily wastewater treatment, Sep. Purif. Technol. 51 (2006) 80–84.

[36] N. Tahri, I. Jedidi, S. Cerneaux, M. Cretin, R. Ben Amar, Development of an asymmetric carbon microfiltration membrane: Application to the treatment of industrial textile wastewater, Sep. Purif. Technol. 118 (2013) 179–187.
[37] I. Jedidi, S. Khemakhem, A. Larbot, R. Ben Amar, Elaboration and characterisation of fly ash based mineral supports for microfiltration and ultrafiltration membranes, Ceram. Int. 35 (2009) 2747–2753.
[38] M.A. Anderson, M.J. Gieselmann, Q.Y. Xu, Titania and alumina ceramic membranes, J. Membr. Sci. 39 (1988) 243–258.
[39] M.S. Strano, A.L. Zydney, H. Barth, G. Wooler, H. Agarwal, H.C. Foley, Ultrafiltration membrane synthesis by nanoscale templating of porous carbon, J. Membr. Sci. 198 (2002) 173–186.
[40] M.S. Strano, H. Agarwal, J. Pedrick, D. Redman, H.C. Foley, Templated pyrolytic carbon: The effect of poly (ethylene glycol) molecular weight on the pore size distribution of poly(furfuryl alcohol)-derived carbon, Carbon 41 (2003) 2501–2508.
[41] G. Wolansky, A. Marmur, Apparent contact angles on rough surfaces: The Wenzel equation revisited, Colloids Surf., A: Physicochem. Eng. Aspects 156 (1999) 381–388.
[42] A. Marmur, Soft contact: Measurement and interpretation of contact angles, Soft Matter 2 (2006) 12–17.
[43] R. Jeffrey, M. Cutcheona, M. Elimelech, Influence of membrane support layer hydrophobicity on water flux in osmotically driven membrane processes, J. Membr. Sci. 318 (2008) 458–466.
[44] B. Tansel, W.Y. Bao, I.N. Tansel, Characterization of fouling kinetics in ultrafiltration systems by resistances in series model, Desalination 129 (2000) 7–14.
[45] B. Van der Bruggen, G. Cornelis, C. Vandecasteele, I. Devreese, Fouling of nanofiltration and ultrafiltration membranes applied for wastewater regeneration in the textile industry, Desalination 175 (2005) 111–119.
[46] E.R. Cornelissen, T.V.D. Boomgaard, H. Strathmann, Physicochemical aspects of polymer selection for ultrafiltration and microfiltration membranes, J. Membr. Sci. 138 (1998) 283–289.
[47] W. Han, H.P. Gregor, E.M. Pearce, Interaction of proteins with ultrafiltration membranes: Development of a nonfouling index test, J. Appl. Polym. Sci. 77 (2000) 1600–1606.
[48] A.L. Ahmad, N.H. Mat Yasin, C.J.C. Derek, J.K. Lim, Chemical cleaning of a cross-flow microfiltration membrane fouled by microalgal biomass, J. Taiwan Inst. Chem. Eng. 45 (2014) 233–241.
[49] A. Simon, J.A. McDonald, S.J. Khan, W.E. Price, L.D. Nghiem, Effects of caustic cleaning on pore size of nanofiltration membranes and their rejection of trace organic chemicals, J. Membr. Sci. 447 (2013) 153–162.